Spatial filtering of audible sound with acoustic landscapes

Shuping Wang,[1,a)] Jiancheng Tao,[1,b)] Xiaojun Qiu,[2,c)] and Jianchun Cheng[1,d)]
[1]*Key Laboratory of Modern Acoustics and Institute of Acoustics, Nanjing University, No. 22 Hankou Road, Nanjing 210093, China*
[2]*Centre for Audio, Acoustics and Vibration, Faculty of Engineering and IT, University of Technology Sydney, PO Box 123, Broadway, NSW 2007, Australia*

(Received 16 March 2017; accepted 8 July 2017; published online 25 July 2017)

Acoustic metasurfaces manipulate waves with specially designed structures and achieve properties that natural materials cannot offer. Similar surfaces work in audio frequency range as well and lead to marvelous acoustic phenomena that can be perceived by human ears. Being intrigued by the famous Maoshan Bugle phenomenon, we investigate large scale metasurfaces consisting of periodic steps of sizes comparable to the wavelength of audio frequency in both time and space domains. We propose a theoretical method to calculate the scattered sound field and find that periodic corrugated surfaces work as spatial filters and the frequency selective character can only be observed at the same side as the incident wave. The Maoshan Bugle phenomenon can be well explained with the method. Finally, we demonstrate that the proposed method can be used to design acoustical landscapes, which transform impulsive sound into famous trumpet solos or other melodious sound. *Published by AIP Publishing*. [http://dx.doi.org/10.1063/1.4995966]

Metasurfaces manipulate waves with specially designed structures and achieve properties that natural materials cannot offer.[1–6] Acoustic metasurfaces of subwavelength thickness provide many kinds of wave manipulation such as acoustic one-way transmission,[7–9] negative refraction of sound waves,[10] acoustic cloaking,[11–13] and so on.[14–19] Periodic corrugated surfaces consisting of steps with sizes comparable to the wavelength of audible sound can be considered as equivalents of metasurfaces in audible frequency range, which lead to a lot of marvelous acoustic phenomena. For example, the steps in front of the Southern Jiangsu Victory Monument can produce 6 bugle-like notes as a result of a firecracker being set off.[20,21] Similar phenomena exist in the El Castillo pyramid, where a sound echo like the chip of a Quetzal bird is produced in response to a handclap and observers hear pulses that sound like raindrops falling in a water filled bucket when other people are climbing the pyramid higher up.[22]

Theories like Fresnel-Kirchhoff diffraction, Bragg reflection, leaky Rayleigh waves, acoustic negative reflection, and the finite element method have been used to investigate these phenomena;[20–25] however, none of the previous work reports an accurate theoretical solution to the scattered sound field either in the frequency or time domain. The mechanisms and physical images of these kinds of large scale metasurfaces are not clear, and there is no approach or procedure reported in previous works to design such a landscape to generate specified sound.

In this letter, we propose an analytical method to calculate the sound field scattered by a periodic corrugated surface and obtain some physical insights into the problem. Numerical simulations and experiments are carried out to demonstrate its validity. We investigate the spatial distribution of the fundamental frequency of scattered sound and its relations to the step sizes. Finally, two acoustical landscapes are designed based on the proposed method which turn impulsive sound into famous trumpet solos and prove that audible sound can be manipulated by artificial surfaces. Our proposed method extends metasurfaces to the audio frequency range and provides the possibility to design interesting acoustical landscapes which have promising applications.

Figure 1(a) is a schematic diagram of such an acoustical landscape which consists of N groups of steps of different sizes. A series of N notes can be heard at the position of the listener in response of an impulse at the position of the source. Figure 1(b) is a cross-sectional view of one of the groups of steps.

According to the Kirchhoff-Helmholtz equation, sound scattered by the surface can be expressed as an integral over the surface A (the surface of the steps)[26,27]

$$p_s = \int_A \left[G \frac{\partial p}{\partial \boldsymbol{n}} - p \frac{\partial G}{\partial \boldsymbol{n}} \right] ds, \tag{1}$$

where G is the Green's function in semi-infinite space and $\boldsymbol{n}$ is the normal vector on the surface. Once the total sound pressure p on the surface is obtained, the scattered sound can be calculated (see the supplementary material for the more detailed process).

We applied the theoretical method on two examples to demonstrate its feasibility. The first one is 10 steps of the size $h = 0.125$ m and $l = 0.315$ m. The theoretical scattered sound pressure level calculated in frequency domain is shown in Fig. 2(a). We can see that the steps work as a frequency-selective filter and the passband and its harmonics is around 534 Hz. The wavelength of the fundamental frequency ($340/534 = 0.64$ m) is about twice the dimensions of the steps ($h = 0.125$ m, $l = 0.315$ m, and $L = 0.339$ m). The boundary element model of the steps was created in ANSYS 14.5 and imported into Sysnoise 5.6, a commercial boundary

[a)]Electronic mail: wangsp822105@126.com
[b)]Author to whom correspondence should be addressed: jctao@nju.edu.cn
[c)]Electronic mail: Xiaojun.Qiu@uts.edu.au
[d)]Electronic mail: jccheng@nju.edu.cn

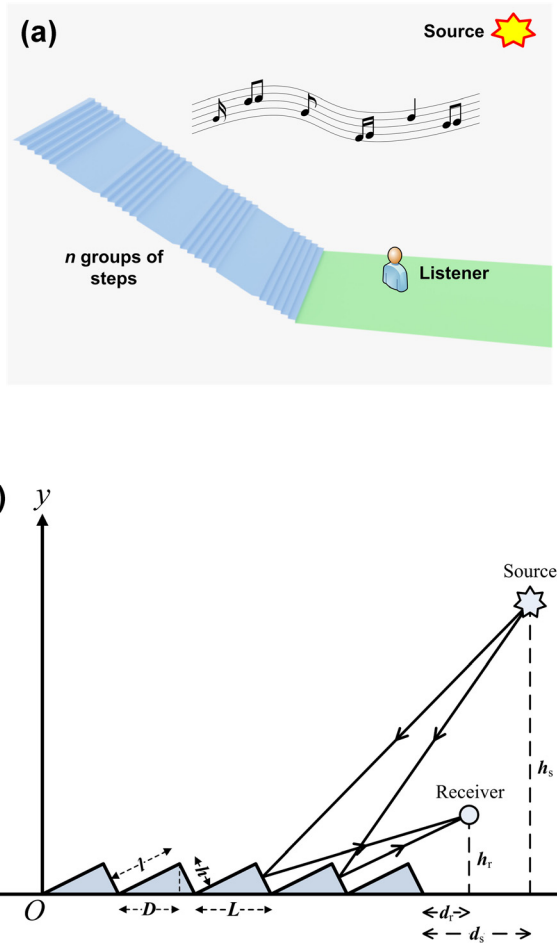

FIG. 1. (a) Schematic diagram of an acoustical landscape consisting of steps. (b) Cross-sectional view of a group of periodic steps. The length and height of each step is l and h, respectively, and the surfaces of the steps are rigid. The distance between the steps and source is d_s along the x axis, and the distance between the steps and receiver is d_r along the x axis. The height of the source and receiver is h_s and h_r, respectively.

element software to obtain the simulation scattered sound pressure, and the results are also shown in Fig. 2(a), which agrees well with theoretical results at most frequencies below 3000 Hz.

We carried out experiments in the anechoic chamber of Nanjing University to further demonstrate simulation results. The experimental setup is indicated in Fig. 2(b). 10 steps of the same length and height as in the above simulations are constructed with boards, and the width is 3.0 m. In the experiments, the starting pistol was used to generate an impulse that is sufficiently short in time domain so that sound scattered by the steps can be separated from direct sound and that reflected from the baffle. A B&K PULSE 3560B analyzer was used to record the signal at the position of the receiver. The recorded signal in time domain is shown in Fig. 2(c). The signal shown in the green box is the direct and reflected sound, and sound scattered by the steps is shown in the red box. The time delay between the direct and scattered sound is about 0.013 s which corresponds to the difference of the length of acoustic paths (about 4.5 m). The power spectral density of the scattered sound in the red box is also indicated in Fig. 2(c). The fundamental frequency of the experimental scattered sound is about 544 Hz, and the error with that predicted by the proposed method (534 Hz) is 1.87%.

After transforming the theoretical scattered sound from frequency to time domain and convolving with the recorded impulse of the starting pistol, we obtain the theoretical time domain signal, and it is shown in Fig. 2(c), as well as the power spectral density of the scattered sound. It is observable that the theoretical scattered signal agrees well with experimental results in both frequency and time domains.

Another example we investigate is the Mount Maoshan model (see Fig. S1 in the supplementary material for the picture of Mount Maoshan monument site and the cross-sectional view of the steps). There are 6 groups of steps, and the steps in the same group have about the same sizes which are listed in Table S1 in the supplementary material. Fundamental frequencies of the sound scattered by each of the 6 groups of steps obtained by applying the proposed method are listed in Table I. The numerical simulation method was also applied on this example by using Odeon 11.23, a room acoustics software, and the results, as well as the measured results, are listed in Table I. It is clear that the fundamental frequencies obtained with the proposed method, Odeon, and measurements agree well with each other, and the maximum error is 4.35%. We also compared the theoretical and recorded scattered sound signal in the time domain (listen to "maoshan_record.wav" and "maoshan_simulation.wav" in the supplementary material) which sound similarly and proves the validity of the proposed method.

The acoustic characters of periodic steps are further investigated by using the proposed method, and two interesting phenomena are observed. First, the maximum scattered sound pressure level at a certain frequency appears within a certain direction at the same side as the incident wave. Figures 3(a) shows the incident sound field when the point source is located at (8.89, 2.00) m, which is marked as a star. Figures 3(b)–3(d) show the distribution of scattered sound pressure level within the area $-6\,\text{m} < x < 10\,\text{m}$, $0\,\text{m} < y < 3\,\text{m}$ at different exciting frequencies (500 Hz, 600 Hz, and 700 Hz). 10 steps are located from $x = 0\,\text{m}$ to $x = 3.39\,\text{m}$ as indicated in Fig. 1(b). The length of each step is 0.315 m, and the height is 0.125 m. In Figs. 3(b)–3(d), the area where maximum sound pressure level appears is near the space indicated by the arrow, which is at different directions at different exciting frequencies; besides, this area is always at the same side as the incident wave.

Second, the fundamental frequencies of scattered sound field have a spatial distribution. Figure 4(a) shows the fundamental frequencies at different locations when the sound source is fixed at (63.16, 70) m, and 10 steps of size $h = 0.1\,\text{m}$, $l = 0.3\,\text{m}$ are located from $x = 0\,\text{m}$ to $x = 3.16\,\text{m}$. We can see that the fundamental frequency increases with x (d_r) and decreases with y (h_r) which indicates a spatial filtering mechanism here. Of course, the fundamental frequency of sound scattered by periodic steps is also related to the size of the steps (h and l). Figure 4(b) shows the fundamental frequencies of scattered sound when the dimensions of the steps (h and l) change, while the relative positions of the sound source and receiver to the 10 steps are fixed ($d_s = 60\,\text{m}$, $h_s = 70\,\text{m}$, $d_r = 30\,\text{m}$, $h_r = 35\,\text{m}$). We can find that the fundamental frequency decreases with either h or l.

Besides predicting the sound field scattered by periodic corrugated steps, we can apply the proposed method to design acoustical landscapes. Theoretically, every kind of

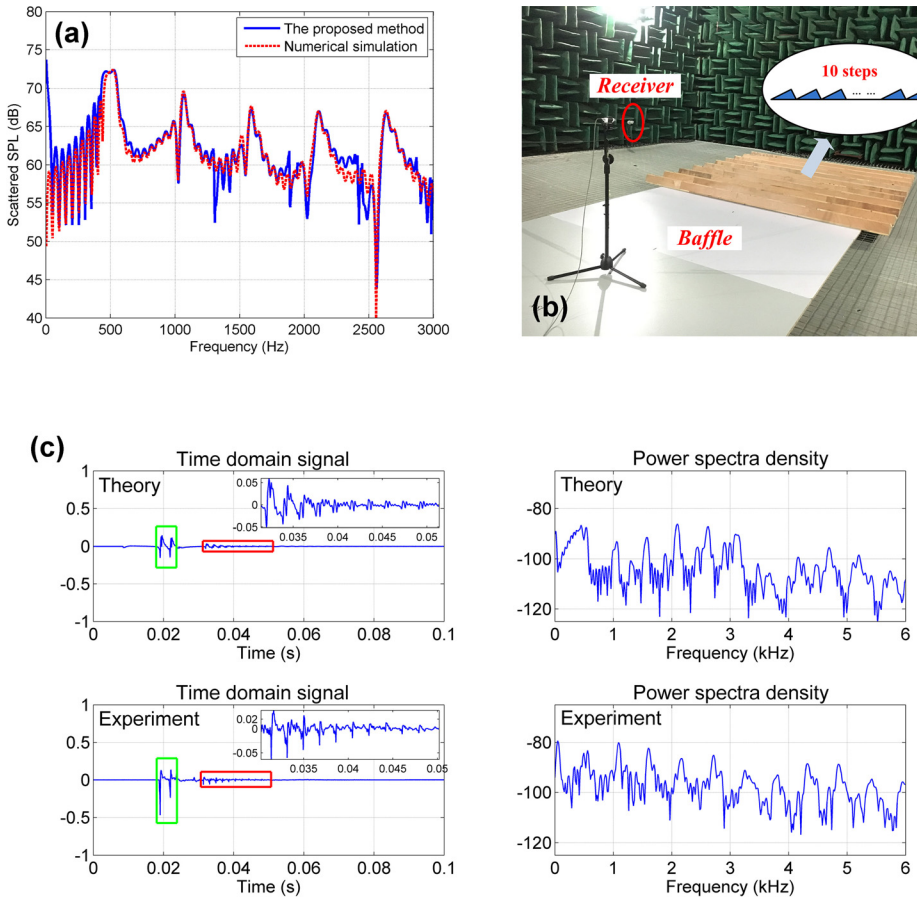

FIG. 2. (a) The scattered sound pressure level (SPL) obtained by the proposed theoretical method and numerical simulations. $d_s = 5.5\,\mathrm{m}$, $h_s = 2.0\,\mathrm{m}$, $d_r = 2.0\,\mathrm{m}$, and $h_r = 1.0\,\mathrm{m}$. (b) The experimental setup in the anechoic chamber. (c) The theoretical and experimental scattered signals in time domain and its power spectral density.

sound can be generated at a certain location by careful design of the metasurfaces and exciting signal. The detailed procedure is as follows:

(1) Analyze the desired sound to be generated by the surfaces and obtain the fundamental frequencies. If there are N notes, there should be N groups of steps.
(2) Choose positions of the sound source and the listener. As mentioned above, periodic steps work as spatial filters and the fundamental frequencies of scattered sound vary at different locations. The sound source and listener must be at the same side of the steps.
(3) Start from the step group nearest to the sound source and listener. Estimate the initial size of the steps (h and l) with

$$l = \frac{c_0}{2f_0}, \tag{2}$$

$$h = \frac{l}{3}, \tag{3}$$

where c_0 is the sound speed and f_0 is the desired fundamental frequency.
(4) Calculate the response in the frequency domain using the proposed method and then transfer it to time domain by

TABLE I. The fundamental frequency of the sound scattered by the 6 groups of steps obtained by the proposed method, Odeon simulation, and measurements.

	Group No.					
The fundamental frequency (Hz)	1	2	3	4	5	6
The proposed method	407	380	368	568	558	427
Odeon simulation	399	368	363	565	554	424
Measurements	416	384	368	560	552	424

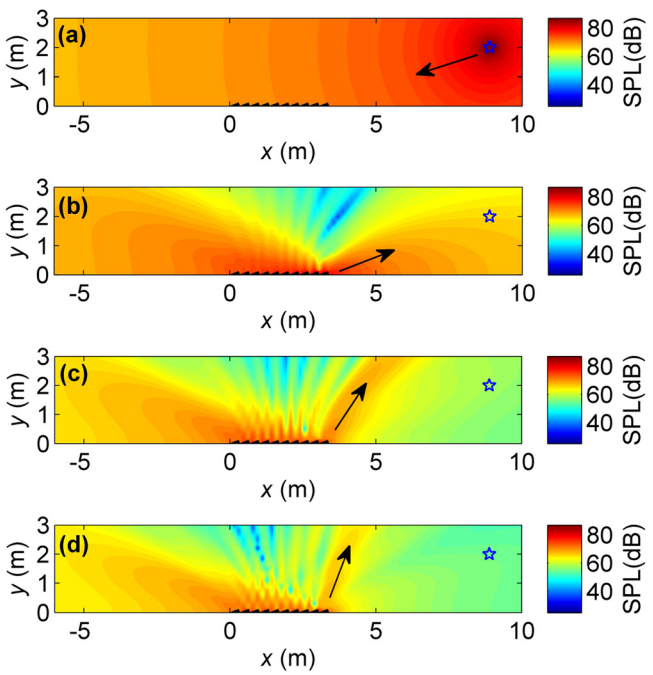

FIG. 3. The distribution of the incident and scattered sound pressure level within the area $-6\,\mathrm{m} < x < 10\,\mathrm{m}$, $0\,\mathrm{m} < y < 3\,\mathrm{m}$ where the sound source is marked as a star. (a) Incident sound. (b) Scattered sound at 500 Hz. (c) Scattered sound at 600 Hz. (d) Scattered sound at 700 Hz.

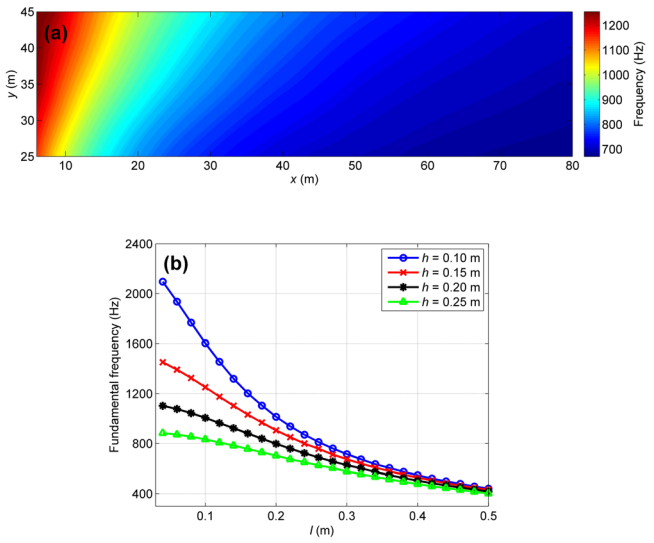

FIG. 4. (a) The spatial distribution of fundamental frequency within the area $6\,\text{m} < x < 80\,\text{m}$, $25\,\text{m} < y < 45\,\text{m}$ when the sound source is fixed at (63.16, 70) m and 10 steps of size $h = 0.1\,\text{m}$, $l = 0.3\,\text{m}$ are located from $x = 0\,\text{m}$ to $x = 3.16\,\text{m}$. (b) The fundamental frequencies of the scattered sound pressure when $h = 0.1\,\text{m}$, $l = 0.3\,\text{m}$, $d_s = 60\,\text{m}$, and $h_s = 70\,\text{m}$.

inverse Fourier transformation, or directly simulate the impulse response using commercial acoustic softwares such as Odeon.

(5) Calculate the scattered sound in time domain by convolving the impulse response with an exciting signal and adjust the parameters h and l with listening tests until the note sounds satisfying.

(6) Repeat the process for the rest of the groups using similar procedure as that for the first group. The distance (ΔL) from the current to the previous step group needs to be estimated first with the time interval t between two notes by $\Delta L = c_0 t/2$. This will determine the distance from the group to the sound source (d_s). With this initial value, we can apply the same procedure as mentioned earlier in Steps 3–5 to obtain the parameters of each group. The parameters ΔL, h, and l need to be adjusted simultaneously with listening tests until all the notes and the time intervals between them sound satisfying.

Two trumpet solos are designed as examples: "Toreador song" and "Neapolitan dance." They consist of 10 and 8 notes, respectively, and the fundamental frequencies of the notes are listed in Tables S2 and S3 in the supplementary material. The proposed method is used to design the size of each step group and the distance between them [The model of the steps is indicated in Fig. 1(a)]. The optimized parameters of the steps are listed in Tables S2 and S3 as well. The designed models are created in SketchUp 8 and imported into Odeon 11.23 to obtain the scattered sound in time domain. The source is 60 m and the listener is 58 m away from the nearest step group in the x direction. The height of the source and listener is 70 m and 35 m, respectively. The simulated scattered signals in time domain are "Toreador_song_simulation.wav" and "Neapolitan_dance_simulation.wav," which sound similarly to the original music "Toreador_song_record.wav" and "Neapolitan_dance_record.wav."

In summary, we propose a theoretical method which can be used to calculate the sound field scattered by a structure consisting of periodic corrugated steps. The feasibility of the method is demonstrated by numerical simulations and experiments. The model is two-dimensional, but it can be used to predict fundamental frequencies of the sound scattered by three-dimensional steps with much less computation load. (The error between fundamental frequencies obtained from two-dimensional and three dimensional model is 0.37%; see the supplementary material.) Although similar phenomena exist in nature, it is the first time that a theoretical model is proposed to describe it in both space and time domains. By using the proposed method, we find that periodic steps work as spatial filters and the scattered sound is different at different positions with the same exciting signal. We also propose a procedure to design interesting acoustical landscapes which is ready for real applications. With comparable size to the wavelength of audio frequencies, such a structure leads to marvelous acoustic phenomena which can be perceived by human ears.

See supplementary material for the detailed process of calculating scattered sound field and the recorded and simulation wav files.

This work was supported by the National Natural Science Foundation of China (Grant Nos. 11474163 and 11634006). The authors would also like to thank Mr. Kang Wang for his help with Odeon simulations.

[1]R. Shelby, D. Smith, and S. Schulta, Science **292**, 77 (2001).
[2]D. Sun, Q. He, S. Xiao, Q. Xu, X. Li, and L. Zhou, Nat. Mater. **11**, 426 (2012).
[3]A. Kildishev, A. Boltasseva, and V. Shalaev, Science **339**, 1232009 (2013).
[4]L. Huang, X. Chen, H. Muhlenbernd, H. Zhang, S. Chen, B. Bai, Q. Tan, G. Jin, K. Cheah, C. Qiu, J. Li, T. Zentgraf, and S. Zhang, Nat. Commun. **4**, 2808 (2013).
[5]A. High, R. Devlin, A. Dibos, M. Polking, D. Wild, J. Perczel, N. Leon, M. Lukin, and H. Park, Nature **522**, 192 (2015).
[6]N. Kaina, F. Lemoult, M. Fink, and G. Lerosey, Nature **525**, 77 (2015).
[7]B. Liang, B. Yuan, and J. Cheng, Phys. Rev. Lett. **103**, 104301 (2009).
[8]Y. Zhu, X. Zou, B. Liang, and J. Cheng, Appl. Phys. Lett. **107**, 113501 (2015).
[9]Y. Zhu, X. Zou, B. Liang, and J. Cheng, Appl. Phys. Lett. **106**, 173508 (2015).
[10]V. Garcia-Chocano, J. Christensen, and J. Sanchez-Dehesa, Phys. Rev. Lett. **112**, 144301 (2014).
[11]M. Farhat, S. Guenneau, and S. Enoch, Phys. Rev. Lett. **103**, 024301 (2009).
[12]Y. Chen, X. Liu, and G. Hu, Sci. Rep. **5**, 15745 (2015).
[13]Y. Cheng, F. Yang, J. Xu, and X. Liu, Appl. Phys. Lett. **92**, 151913 (2008).
[14]Y. Xie, W. Wang, H. Chen, A. Konneker, B. Popa, and S. Cummer, Nat. Commun. **5**, 5553 (2014).
[15]M. Moleron and C. Daraio, Nat. Commun. **6**, 8037 (2015).
[16]A. Marzo, S. Seah, B. Drinkwater, D. Sahoo, B. Long, and S. Subramanian, Nat. Commun. **6**, 8661 (2015).
[17]G. Ma, M. Yang, S. Xiao, Z. Yang, and P. Sheng, Nat. Mater. **13**, 873 (2014).
[18]Y. Cheng, C. Zhou, B. Yuan, D. Wu, Q. Wei, and X. Liu, Nat. Mater. **14**, 1013 (2015).
[19]J. Zhao, H. Ye, K. Huang, Z. Chen, B. Li, and C. Qiu, Sci. Rep. **4**, 6257 (2014).
[20]C. Xu, M. Qin, S. Wang, and H. Zhou, Am. J. Phys. **82**, 135 (2014).

[21]Z. Yang, X. Wang, and J. Zhang, J. Nanjing Univ. (Nat. Sci.). **51**, 1097 (2015).
[22]N. Declercq, J. Degrieck, R. Briers, and O. Leroy, J. Acoust. Soc. Am. **116**, 3328 (2004).
[23]N. Declercq and C. Dekeyser, J. Acoust. Soc. Am. **121**, 2011 (2007).
[24]N. Declercq, J. Degrieck, and O. Leroy, J. Appl. Phys. **98**, 113521 (2005).
[25]T. Nicolas, L. Sylvain, D. Carsten, and D. Matteo, "19th International Congress on Acoustics," in Proceedings of a meeting held 2–7 September 2007 (SEA, Madrid, 2007).
[26]P. Morse and K. Ingard, *Theoretical Acoustics* (MacMillan, London, 1986).
[27]J. Cheng, *The Principle of Acoustics* (Chinese Edition) (Science Press, Beijing, 2012).